# An Isothermal Microcalorimeter with Integrated $CO_2$ Sensor for Simultaneous Measurement of Microbial Heat Evolution and Mineralization

Shiyue Yang[1], Sven Paufler[1], Hauke Harms[2], Matthias Kästner[3], Anja Miltner[3], Thomas Maskow[1*]

[1]Department of Microbial Biotechnology, Helmholtz-Centre for Environmental Research – UFZ, Permoserstraße 15, 04318 Leipzig, Germany

[2]Department of Applied Microbial Ecology, Helmholtz-Centre for Environmental Research – UFZ, Permoserstraße 15, 04318 Leipzig, Germany

[3]Department of Molecular Environmental Biotechnology, Helmholtz-Centre for Environmental Research – UFZ, Permoserstraße 15, 04318 Leipzig, Germany

Corresponding author: Thomas Maskow, thomas.maskow@ufz.de

**Keywords:** Calorimetry, respirometry, calorespirometric ratio, soil, $CO_2$ sensor

## Abstract

Soil, as the largest terrestrial carbon sink, plays a crucial role in carbon sequestration. Within soil systems, microorganisms decompose soil organic matter to generate energy and obtain carbon for growth, concomitantly release heat and $CO_2$ as metabolic byproducts. The calorespirometric (CR) ratio – defined as the ratio of heat production to $CO_2$ evolution, is a key indicator of carbon use efficiency and soil anaerobicity. However, conventional methodologies typically measure heat and $CO_2$ separately, with $CO_2$ often quantified by intermittent sampling. This discontinuous approach, compounded by the inherent heterogeneity of soil, introduces uncertainties in calorespirometric analysis. To address this limitation, an infrared $CO_2$ sensor was mounted onto a stainless-steel calorimetric ampoule, containing soil-glucose mixtures, enabling simultaneous real-time measurements within an isothermal microcalorimeter. The novel configuration permits continuous monitoring of both parameters, validated through comparative analysis with traditional methods. The derived CR ratio aligned with theoretical predictions for carbohydrates metabolism. Furthermore, parallel oxygen measurements enabled quantification of CR ratio based on $O_2$ (heat-to-$O_2$), and the respiratory quotient ($CO_2$-to-$O_2$)), offering deeper insight into microbial carbon-energy coupling and turnover in soil systems. This methodological advancement enhances the capacity to interrogate soil biogeochemical processes under dynamic environmental conditions.

# Graphical Abstract

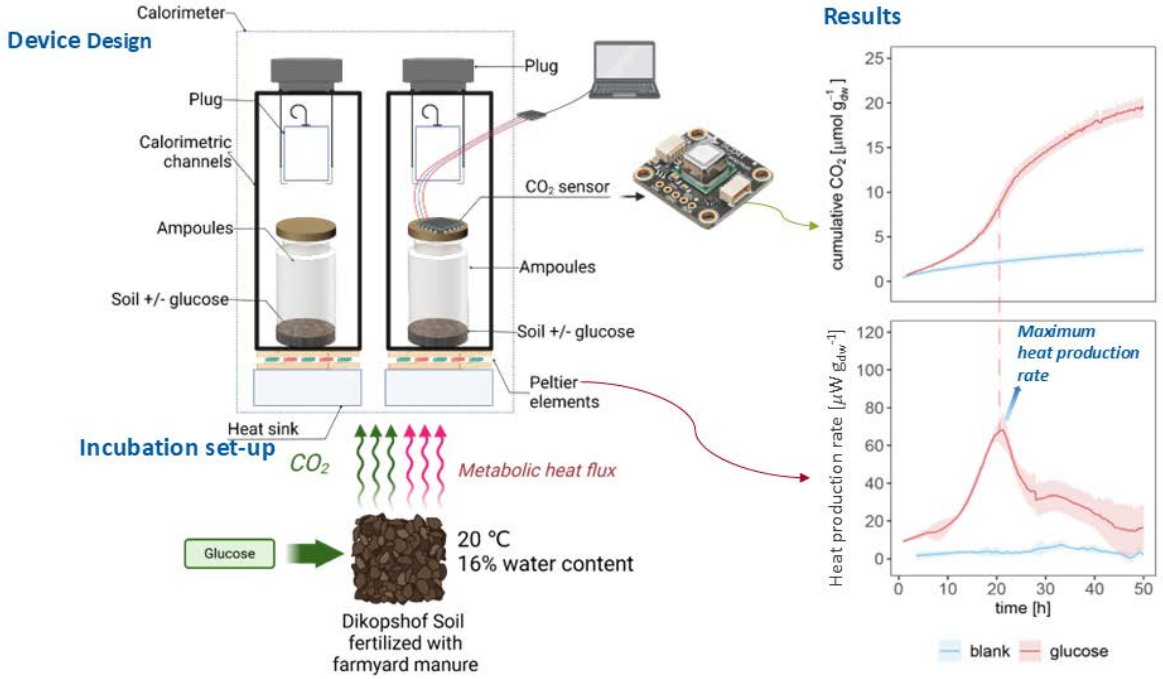

# List of Symbols

| Symbol | Property | Unit |
|---|---|---|
| $CO_2(t)$ | Cumulative $CO_2$ amount at time $t$ | mol $g_{dw}^{-1}$ |
| CER | $CO_2$ evolution rate at time $t$ | mol $g_{dw}^{-1}$ $d^{-1}$ |
| $CR_{CO_2}(t)$ | Calorespirometric ratio based on $CO_2$ production at time $t$ | J $mol^{-1}$ |
| $CR_{O_2}(t)$ | Calorespirometric ratio based on $O_2$ consumption at time $t$ | J $mol^{-1}$ |
| dw | Dry weight | g |
| $O_2(t)$ | $O_2$ consumption amount at time $t$ | mol $g_{dw}^{-1}$ |
| $P$ | Atmospheric pressure | Pa |
| $P_m(t)$ | Specific heat production rate | W $g_{dw}^{-1}$ |
| $P_{SG}(t)$ and $P_S(t)$ | Specific heat production rate for soil amended with glucose and control at time $t$ | W $g_{dw}^{-1}$ |
| $Q_m(t)$ | Specific total heat | J $g_{dw}^{-1}$ |
| $Q_{SG}(t)$ and $Q_S(t)$ | Specific total heat for soil amended with glucose and control at time $t$ | J $g_{dw}^{-1}$ |
| $R$ | Gas constant | J $mol^{-1}$ $K^{-1}$ |
| $RQ\ (t)$ | Respiratory quotient at time $t$ | mol $mol^{-1}$ |
| $T$ | Temperature | K |
| $t$ | Time point | s |
| $V_{CO_2}$ | Volume of cumulative $CO_2$ in the air space | mL |
| $V_{O_2}$ | Volume of consumed $O_2$ in the air space | mL |
| *WHC* | Water holding capacity | g $g_{dw}^{-1}$ |
| WC | Water content | g $g_{dw}^{-1}$ |
| $\Delta_r H$ | Reaction enthalpy | J $mol^{-1}$ |
| $\Delta t$ | Duration of measurement | s |
| | | |
| **Abbreviations** | **Meaning** | |
| C | Carbon | |
| E | Energy | |
| DFYM | Dikopshof farmyard manure soil | |
| FFT | Fast Fourier Transform | |
| IFFT | Inverse Fast Fourier Transform | |
| IMC | Isothermal microcalorimeter | |
| IR | Infrared | |
| (S)OC | (Soil) Organic carbon | |
| (S)OM | (Soil) Organic matter | |
| | | |
| **subscripts** | **Meaning** | |
| S | Soil | |
| SG | Glucose-amended soil | |
| w | Water | |
| dw | Dry weight | |

# 1. Introduction

A substantial amount of carbon (C) is stored in soil organic matter (SOM) and many compounds are utilized by microorganisms for their metabolism. Heterotrophic organisms gain energy (E) by catabolic reactions and utilize carbon (C) for biosynthesis in anabolism. Combining these processes results in growth and formation of biomass, which finally can contribute to C sequestration in SOM (Chakrawal et al., 2021; Kästner et al., 2024). During microbial metabolism, degraded C thus is either released as $CO_2$ into the atmosphere through respiration or retained and stabilized as biomass or other forms of SOM in the soil. Microbial catabolism provides usable E for anabolism in soil but also generates heat. Both heat and $CO_2$ are critical parameters for quantifying microbial traits in soil systems, as microbes require both matter and E fluxes for growth and maintenance (Herrmann et al., 2014; Chakrawal et al., 2021; Kästner et al., 2024). The calorespirometric (CR) ratio, defined as the quotient between specific heat release ($Q_m$) and cumulative $CO_2$ amount or between heat production rate ($P_m$) and $CO_2$ evolution rate (CER), provides insight into various metabolic pathways and growth (Hansen et al., 2004; Yang et al., 2024; Wirsching et al., 2025). The CR ratio is considered to correlate with carbon use efficiency (CUE), which quantifies the conversion efficiency of ecosystem C inputs into microbial C storage in soil systems (Hansen et al., 2004; Manzoni et al., 2012; Sinsabaugh et al., 2013).

Heat and $CO_2$ are typically measured using separately devices. Microbial metabolic $Q_m$ during soil incubation is conventionally measured using isothermal microcalorimeters (IMCs) such as TAM Air, TAM IV (TA Instruments, New Castle, USA), I-Cal flex IMC (Calmetrix Inc, Sweden) or microcalvet (Seteram, France), which offer capacities ranging from 4 to 20 mL for continuous specific heat production rate ($P_m$) monitoring with parallel measurements in 2-48 channels (Barros et al., 2011; Maskow and Paufler, 2015). Several methods are available for $CO_2$ quantification. Headspace gas sampling followed by gas chromatography quantification is commonly used for discontinuous but highly accurate $CO_2$ quantification (Tiemann and Billings, 2011). As an alternative, $CO_2$ can be trapped in NaOH solution and quantified by titration. This approach is widely followed, though it does not support real-time, online measurement (Jing et al., 2022; Kabwe et al., 2022). Respirometers are useful devices for quantifying $CO_2$ production rate by measuring the decrease in the conductance of a KOH solution caused by sorption of $CO_2$ produced during incubation; these instruments are suitable for large soil samples (Nordgren, 1988; Endress et al., 2024). However, the conductimetric sensors used in these systems are temperature-sensitive and require a stable thermostat for accurate operation (Satienperakul et al., 2004). Additionally, $CO_2$ measurement after sorption into NaOH or KOH traps might introduce detection delays due to the diffusion of released $CO_2$ into the alkaline solution (Endress et al., 2024). Another alternative is to apply a colorimetric method, which determines $CO_2$ respiration through the changes in pH in a dilute bicarbonate solution containing a pH indicator dye. This approach, based on alkali absorption, is considered to be convenient but less accurate than methods mentioned above (Rowell, 1995). However, the discontinuous and separate measurement of heat and respiration complicates the accurate coupling of C and E dynamics and may introduce bias due to the complex and heterogeneous nature of soil matrix.

Several attempts have been made to quantify $CO_2$ and heat simultaneously using several different methods (Barros et al., 2008; Herrmann and Bölscher, 2015; Wadsö, 2015; Wadsö and Hansen, 2015; Yang et al., 2024). One approach involved combining a twin-flow microrespirometer and a calorimeter in an open-flow system to study the ecophysiology of aquatic organisms (Gnaiger, 1989). Another widely used method integrates the $CO_2$-trapping solution into calorimetric ampoules, relying on the absorption reaction between NaOH and $CO_2$. This technique has been applied to soil systems or plant tissues (Criddle et al., 1990; Barros and Feijóo, 2003; Barros et al., 2011). The extra absorption heat generated by the sorption of $CO_2$ in the NaOH solution is assumed to be directly proportional to the amount of $CO_2$ produced, allowing for the calculation of $CO_2$ evolution rate (Criddle et al., 1990). However, these alkaline-based methods all depend on the assumption that $CO_2$ absorption by alkaline solution and the resulting reduction in $CO_2$ partial pressure do not alter the soil metabolism. However, recent experiments have shown that the reduced $CO_2$ partial pressure may potentially interfere with microbial growth in soil (Yang et al., 2024). Wadsö et al. (2004) developed a device connecting two isothermal heat conduction calorimeters by a tube, one of which was filled with a $CO_2$ absorbent. This setup enabled simultaneous measurement of heat release and $CO_2$ production by two mould fungi. However, the accuracy of heat measurement exhibits variability, necessitating further technical improvement and enhanced data interpretation for metabolic flux analysis. Herrmann and Bölscher (2015) proposed another method combing the microtiter plate method with calorimetric measurements. In their approach heat disturbance from the sorption between $CO_2$ and bicarbonate was negligible whereas they only measured cumulative $CO_2$ release at the end of an incubation period in soil systems. However, this method lacks information on the kinetics of C and E turnover. Fricke et al. (2024) successfully established a prototype of a calorespirometer by introducing a thermoelectric generator at the bottom of the measuring vessel in an established conductometric respirometer, allowing for simultaneous calorespirometric measurements of E release and $CO_2$ production by yeast growing in a liquid medium, which has not been tested for longer durations.

The goal of our study was to develop a device capable of simultaneously and continuously measuring heat and $CO_2$ from the same soil sample while minimizing effects of $CO_2$ diffusion and soil heterogeneity. We integrated an infrared (IR) $CO_2$ measuring sensor, the SCD41 sensor, directly on top of the calorimetric ampoules. The compact size of this sensor and its precision at $CO_2$ concentrations relevant for soil incubations makes it ideal for incorporation into the IMC systems. We tested the reliability of the sensor after integration into the ampoule caps and the performance of the calorimetric measurements of soil processes with this approach. Simultaneous heat and $CO_2$ measurement were conducted in parallel to analysis of residual $O_2$ saturation by an optical fibre sensor for full evaluation of microbial metabolic pathways. This study presents the design, implementation and experimental validation of the integrated calorespirometric system. This includes measurements of heat release, $CO_2$ evolution, $O_2$ consumption, the calorespirometric ratio ($\mathrm{CR}_{\mathrm{CO_2}}$ and $\mathrm{CR}_{\mathrm{O_2}}$) and respiratory quotient ($\mathrm{RQ}$) from soil amended with glucose.

# 2. Materials and Methods

## 2.1 Soil Preparation

A silt-loam textured soil sampled from the Dikopshof long-term experiment (DFYM) was used for the simultaneous heat and $CO_2$ release measurements. The physicochemical properties of Dikopshof soil are well-characterized (Lorenz et al., 2024). Glucose was selected as an easily degradable substrate for testing our calorespirometric system. The air-dried soil was sieved through 2-mm sieve, with aggregates crushed and stones removed. Water was added to the sieved soil in a glass beaker to reach 14% (g water per g dry water, $g_w\ g_{dw}^{-1}$, approximately 46% of water holding capacity) water content. The glass beaker was then sealed tightly with parafilm, and the soil was pre-incubated at 20 °C for 7 days. After pre-incubation, glucose solution (min. 99%, CHEMSOLUTE, 45 g $L^{-1}$) was added to the soil to reach 16% water content ($g_w\ g_{dw}^{-1}$, approximately 52% water holding capacity) and glucose concentration of 900 $\mu g\ g_{dw}^{-1}$. For the control treatment, deionized water was added to pre-incubated soil to reach the same water content ($g_w\ g_{dw}^{-1}$). In each round of experiment, around 2.18 g of either glucose- or non- amended soil (equalling to approximately 1.88 g dry weight) per calorimetric channel was transferred to a 20-mL stainless-steel ampoule, with a top screw lid designed for static and air-tight calorimetric experiments. Each treatment was performed in triplicate and monitored continuously for approximately 50 hours.

## 2.2 Set-up for the Simultaneous Measurement of Heat and $CO_2$

The IMC used in this experiment, TAM Air (TA Instrument, New Castle, USA), equipped with eight measuring and reference channels, was utilized for simultaneous heat and $CO_2$ measurement. The SCD41 sensor (Sensirion, 2021; details provided in Supplementary Materials, SM S1) was mounted on the cap for the stainless-steel vessel, with a customized cut in the lid to fit the sensor. The SCD41 sensor was connected to a microcontroller (Arduino Micro or Pro Micro Atmeg32U4, Arduino, Turin, Italy), which supplied 5 V power to the sensor module and established serial $I^2C$ communication. The microcontroller fetched data from the SCD41 and transferred them to a computer connected via USB for data logging. The microcontroller was placed externally, outside TAM Air channels. The original plastic heat sink plug at the top of calorimetric ampoules were replaced by a rubber plug of same size, allowing the space for cables (37 American Wire Gauge, 37 AWG, Donau Elektronik GmbH, Metten, Germany) to connect the sensor with the microcontroller. The setup for simultaneous heat and $CO_2$ measurements is illustrated in **Fig. 1**. The gas tightness of stainless-steel ampoules was proven by injecting a gas mixture containing around 2.2% $CO_2$ and monitoring the $CO_2$ concentration over 200 h (see **Fig. S1**A). As the $CO_2$ concentration only declined from 2.2% to 2.1% over 200 hours (**Fig. S1**A), we considered the decrease during our experiments as negligible. Potential heat disturbances from the sensor operation were assessed, and these findings are also included in **Fig. S1**B. The heat output of the sensor was relatively constant at $1.6 \pm 0.3$ mW (**Fig. S1**B). The stainless-steel ampoule showed comparable heat measurement behaviour as standard glass calorimetric ampoules.

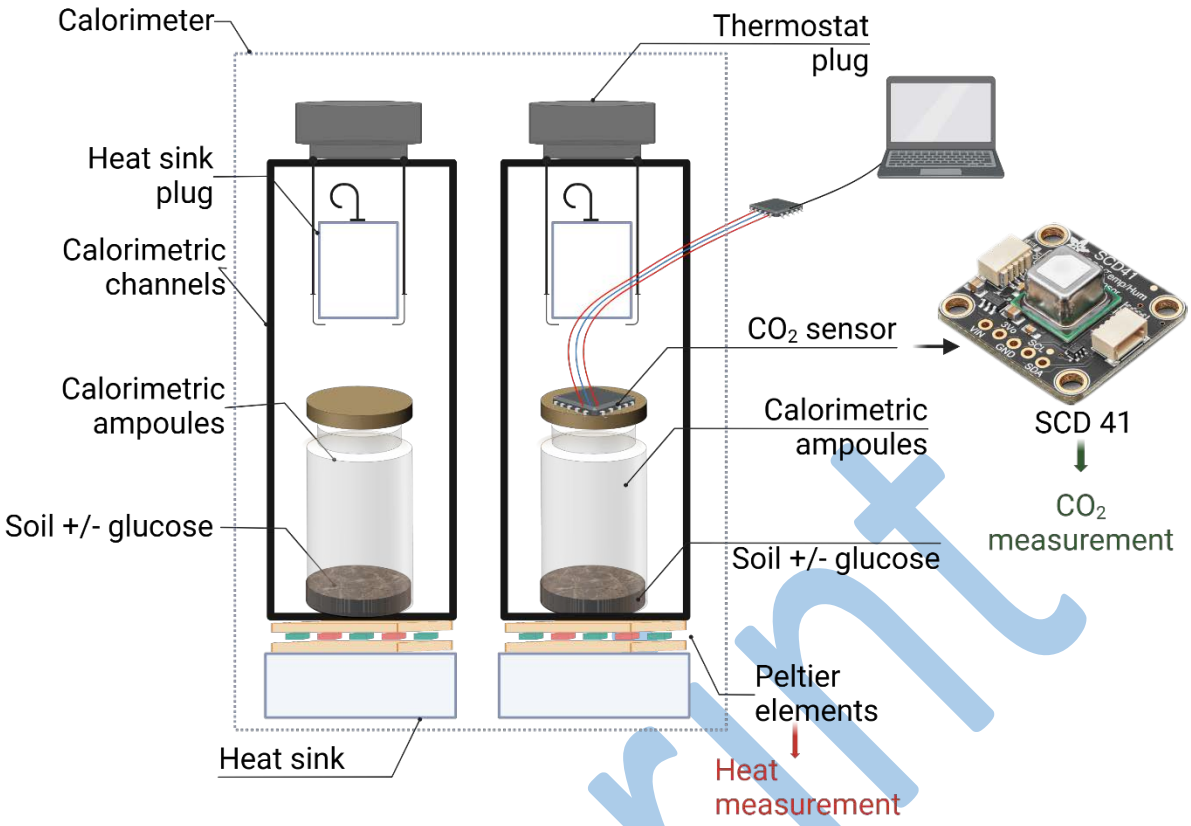


**Figure 1**. Set-up of simultaneous measurement of $P_m(t)$ and cumulative $CO_2$ release. Equal amounts of glucose-amended or non-amended soil were added to an ampoule with a $CO_2$ sensor mounted on top of the ampoule and the ampoule without $CO_2$ sensor mounted on top of the ampoule, respectively, which were then positioned within the channels of the TAM Air (indicated by the bold black lines). The SCD41 sensor continuously monitors cumulative $CO_2$ concentration in the gas space inside of the stainless-steel ampoules.

Finally, the ampoules were sealed using the lid and a rubber ring. To improve gas tightness, a thin layer of silicone grease (GE Bayer Silicones Grease Baysilone Paste Medium Viscosity, 35g, Bayer AG, Leverkusen, Germany) was applied around the lid. The stainless-steel vessel was then carefully inserted into the calorimeter channel. To validate the heat signal, two glass calorimetric ampoules without $CO_2$ sensor and filled with similar amounts of soil were inserted into TAM Air for both non- and glucose-amended soil samples. Reference ampoules were filled with 1.362 mL deionized water which is estimated to have same heat capacity as the soil samples. Before inserting the ampoules, the heat signal baseline was recorded for 30 minutes, and the mean value of this period was defined as the heat signal baseline. Calorimetric signals were monitored continuously, with the final dataset exported at 5-second intervals. For $CO_2$ measurement, the SCD41 sensor was activated approximately 1 hour prior to incubation. The cumulative $CO_2$ evolution was measured in ppm at 15-minute intervals throughout the experiment, and cumulative $CO_2$ release was calculated from these data. That interval length was chosen to minimize self-heating of the sensor and maintain adequate data resolution.

## 2.3 $O_2$ measurement

In a parallel experimental set-up, $O_2$ concentrations were analysed non-invasively in closed 60-mL vials by optical oxygen sensor spots (SP-PSt7-NAU, PreSens Precision Sensing GmbH, Regensburg, Germany) attached to the inner wall of the vials. The sensor spot was positioned slightly above the soil surface within the vials to ensure accurate monitoring. $O_2$ concentration was monitored at 15-minute intervals at 20 °C. The air/soil ratio in the 60 mL vial was designed to match that of the stainless-steel ampoule used in TAM air, ensuring consistency across experimental conditions.

## 2.4 Data and statistical analysis

A theoretical framework was developed to calculate key parameters and to derive relevant thermodynamic and kinetic parameters of microbial processes based on the simultaneous calorespirometric measurements in our experiments.

In Eq. (1), $P_m(t)$ is the specific heat production rate derived from glucose metabolism and both heat production rate with and without glucose addition were measured and $P_m(t)$ was calculated as the difference between $P_{SG}(t)$ and $P_S(t)$ (SM S3 **Eq.** (S1)). The total metabolic specific heat, $Q_m\ (t)$ was determined by integrating the $P_m(t)$ over time, as expressed in Eq. (1). Analogous to $P_m(t)$, $Q_m\ (t)$ is the difference between the total heat measured from glucose-amended and non-amended soil (SM S3 **Eq.** (S2)).

$$Q_m(t) = \int_{t=0}^{t} P_m(t)\,\mathrm{d}t \qquad \textbf{Eq.}\ (1)$$

The measured $CO_2$ concentrations ($CO_2(t)$) were converted to mol per gram dry weight soil via the ideal gas law according to the **Eq.** (2):

$$\mathrm{CO_2}(t)[\frac{mol}{{g_{dw}}^{-1}}] = \frac{P \cdot V_{\mathrm{CO_2}}}{R \cdot T} \qquad \textbf{Eq.}\ (2)$$

Where $P$ (101 325 Pa) represents the atmospheric pressure, $V_{CO_2}$(mL) is the calculated $CO_2$ partial volume in the reaction vessel, $R$ (8.314 [J mol$^{-1}$ K$^{-1}$]) is the gas constant, and $T$ (20 °C, 293.15 K) is the temperature. The equation to calculate $V_{CO_2}$ is shown in SM S3 **Eq**. (S3) from measured cumulative $CO_2$ evolution [ppm] in the airspace. Finally, the increased concentrations were used to calculate cumulative $CO_2$ production.

The consumed $O_2$ at time = t ($O_2(t)$) was converted to $\mu$mol per gram dry weight soil according to **Eq.** (3) and the volume of consumed $O_2$ ($V_{O_2}$) was calculated via **Eq**. (S4) in SM S3:

$$\mathrm{O_2}(t)[\frac{mol}{{g_{dw}}^{-1}}] = \frac{P \cdot V_{O_2}}{R \cdot T} \qquad \textbf{Eq.}\ (3)$$

The calorespirometric (CR) ratio is a crucial parameter in distinguishing metabolic pathways as it integrates both metabolic heat and respiration dynamic. Different approaches are used in previous studies, based on the quotient between heat release and either $CO_2$ production (**Eq.** (5)) or $O_2$ uptake (**Eq.** (6)) (Hansen et al., 2004).

$$CR_{CO_2}(t) = \frac{Q_m\,(t)}{CO_2(t)} \quad \textbf{Eq.}\ (5)$$

$$CR_{O_2}(t) = \frac{Q_m\,(t)}{O_2(t)} \quad \textbf{Eq.}\ (6)$$

The microbial respiratory quotient ($RQ(t)$) is defined as the ratio of $CO_2$ evolution over $O_2$ uptake and was estimated using **Eq.** (7) (Endress et al., 2024).

$$RQ(t) = \frac{CO_2(t)}{O_2(t)} \quad \textbf{Eq.}\ (7)$$

With the SCD41 sensor present, each measurement produced a certain amount of heat, resulting in periodic noise according to the 15-minute measurement interval. This heat production added up to the metabolic $P_m(t)$. This additional heat must be accounted for when evaluating the raw data. To address the heat interference caused by the IR sensor measurement, a Fast Fourier Transform (FFT) frequency domain analysis followed by an inverse FFT (IFFT) analysis to process the filtered data was performed using R Studio (version 4.3.0). This dual-transformation approach effectively isolated and removed sensor-induced thermal noise. Detailed information of the implementation and parameter specifications are provided in SM S4 (Cooley and Tukey, 1965).

The final $Q_m\,(t)$ at t = 50 hours was compared between samples with sensor and without sensor, for both non-amended and glucose-amended soil treatments to assess the disturbance caused by sensor operation on data accuracy. The comparison was conducted by using a one-way ANOVA with contrasts between treatments regarded significant at a significance level of $\alpha$ = 0.05 with the "stats" package in R (v. 4.3.0, Hirsch, (2024)).

# 3. Results

Glucose was rapidly metabolised after addition to the soil, resulting in a relatively sharp peak of $P_m(t)$ and continuously increasing $CO_2$ concentrations (**Fig. 2**) whereas both $P_m(t)$ and $CO_2$ production remained on a low level in the unamended soil. $P_m(t)$ peaked at approximately 20 hours and stabilized at the metabolic baseline after around 50 hours. $CO_2(t)$ production amount exhibited a similar trend, aligning the accumulated $Q_m\,(t)$ value. The integration of the $CO_2$ sensor into the lids of calorimetric ampoules enabled simultaneous and continuous measurement of metabolic heat release and respiration from the same soil sample, overcoming limitations posed by $CO_2$ diffusion and soil heterogeneity.

## 3.1 The influence of the sensor on metabolic heat measurement

To validate the heat measurement with the SCD41 sensor on top of the ampoule, $P_m$ was measured in glucose-amended and non-amended soil, both with and without the sensor. In non-amended soil, $P_m$ remained relatively constant, averaging at $4 \pm 1$ $\mu$W $g_{dw}^{-1}$ with the sensor and $5 \pm 1$ $\mu$W $g_{dw}^{-1}$ without sensor (**Fig. 2**A). In glucose-amended soil with the sensor, $P_m$ increased over the first 20 hours with a peak at $68 \pm 9$ $\mu$W $g_{dw}^{-1}$ around 21 h, and stabilized at a metabolic baseline of $17 \pm 12$ $\mu$W $g_{dw}^{-1}$ by approximately 50 hours (**Fig. 2**B). Similar trends were observed in standard glass ampoules, with a metabolic peak at $64 \pm 12$ $\mu$W $g_{dw}^{-1}$ at 21

hours (**Fig. 2**B). In non-amended soil, $Q_m$ only showed a slight increase, reaching 0.60±0.03 J $g_{dw}^{-1}$ with the sensor and 0.7±0.2 J $g_{dw}^{-1}$ without the sensor (**Fig. 2**C). The integrated $Q_m$ for glucose-amended soil increased to 5±1 J $g_{dw}^{-1}$ over 50 hours, regardless of whether the sensor was present or not (**Fig. 2**D). Measurements of both $P_m$ and $Q_m$ using the sensor-integrated system aligned closely with those from the systems without sensor, with no significant differences observed in $Q_m$ at 50 hours across both experimental configurations (**Fig. S2**). This consistency demonstrates that the sensor integration did not compromise the accuracy of metabolic heat production measurements, provided that the data were corrected for the heat output of the sensor. In glucose-amended soil with sensor, the error range increased from the peak time until reaching the final metabolic baseline, compared to configurations without the sensor (**Fig. 2**B).

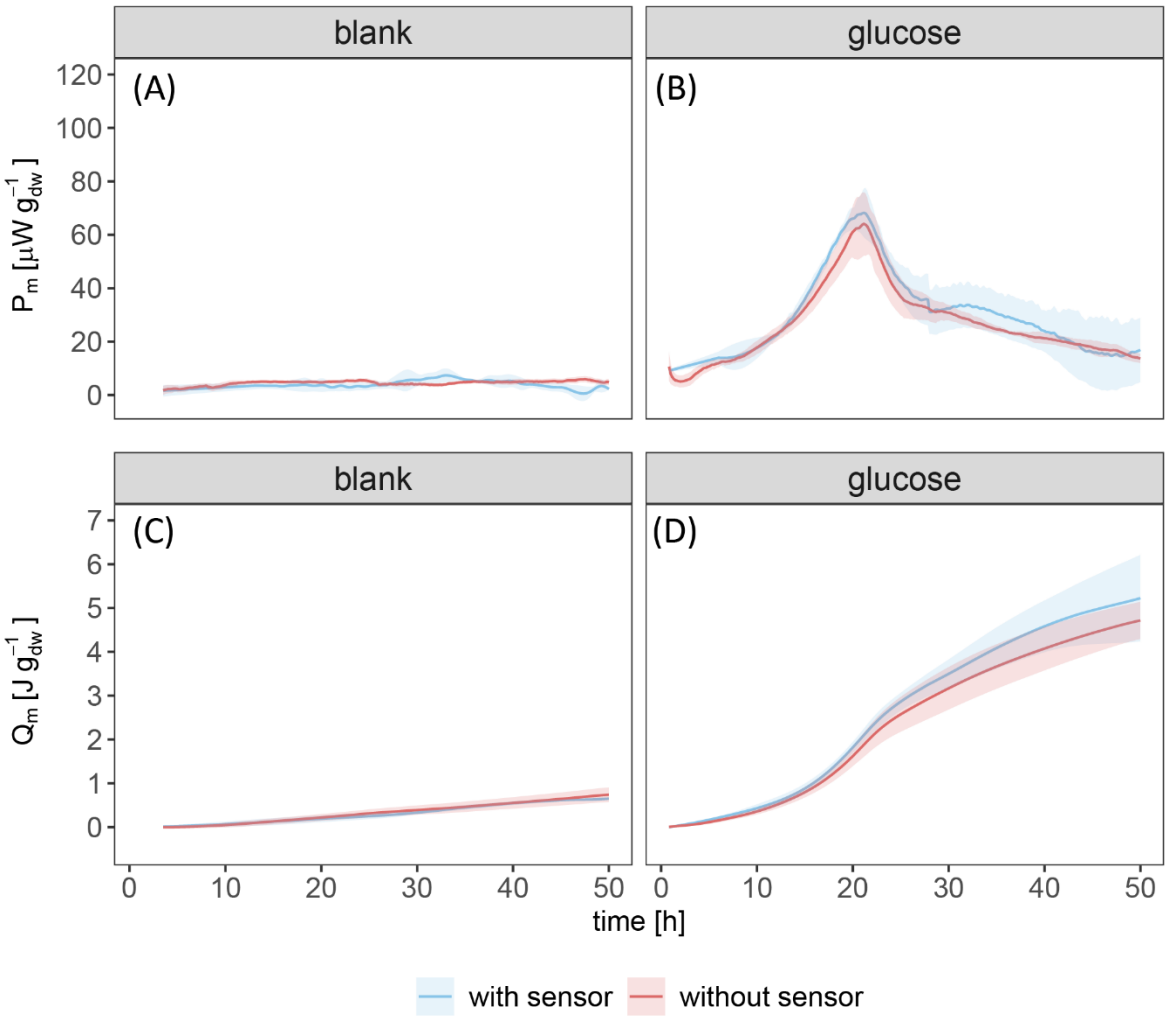


**Figure 2** Metabolic heat production rate ($P_m(t)$, mean ± SD) and integrated heat ($Q_m(t)$, mean ± SD) over 50 hours for non-amended (left panels) and glucose-amended soil (right panels), measured with (blue curves) and without the sensor (pink curves). (A) $P_m$ of non-amended soil with and without the sensor; (B) $P_m$ of glucose-amended soil with and without the sensor; (C) $Q_m$ of non-amended soil with and without the sensor; (D) $Q_m$ of glucose-amended soil with and without the sensor. The shading on both sides of the curves represents standard deviations (n = 3).

### 3.2 $CO_2$ evolution, $O_2$ consumption, calorespirometric ratios and respiratory quotient

During the 50-hour incubation, metabolic $CO_2$ production reached 16±1 $\mu$mol $g_{dw}^{-1}$ for soil with glucose addition while the total $O_2$ consumption was 12±3 $\mu$mol $g_{dw}^{-1}$. As depicted in **Fig. 3**A, $CO_2$ evolution consistently exceeded $O_2$ consumption, with the disparity reaching approximately 5±3 $\mu$mol $g_{dw}^{-1}$ after 50 hours. The RQ increased from 0 to approximately 1.4±0.4 mol $mol^{-1}$ at 21.5 hours, aligning with the peak in $P_m$. Subsequently, RQ stabilized between 1.3 and 1.5 mol $mol^{-1}$ from 21.5 hours to 50 hours (**Fig. 3**B). The calorespirometric ratio based on oxygen consumption ($CR_{O_2}$) fluctuated during the first 10 hours but then increased from 150±170 kJ mol $O_2^{-1}$ to approximately 419±119 kJ mol $O_2^{-1}$, remaining stable at 407±121 kJ mol $O_2^{-1}$ between 30 to 50 hours (**Fig. 3**C). In contrast, $CR_{CO_2}$ (based on $CO_2$ evolution) rose slightly from 247±133 kJ mol $CO_2^{-1}$ to 358±249 kJ mol $CO_2^{-1}$ at around 7 hours, before decreasing to approximately 272±52 kJ mol $CO_2^{-1}$. Between 20 and 50 hours, CR remained relatively stable at around 272±44 kJ mol $CO_2^{-1}$ (**Fig. 3**D).

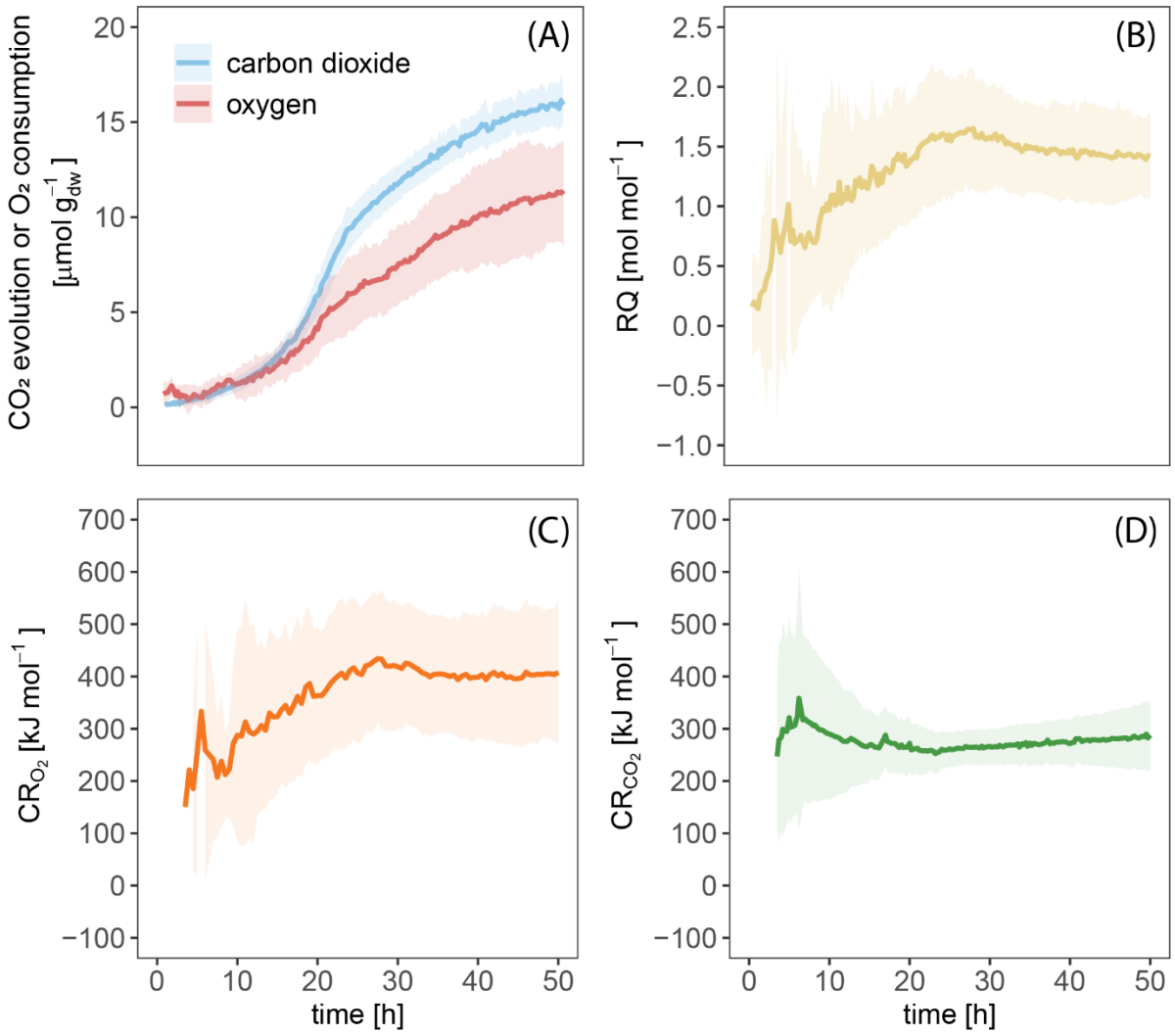


**Figure 3** (A) Cumulative $CO_2$ evolution (blue curves) and $O_2$ consumption (pink curves) over 50 hours of incubation. (B) Dynamics of RQ derived from $CO_2$ evolution and $O_2$ consumption (C) Dynamics of $CR_{O_2}$ calculated from cumulative $Q_m$ and $O_2$ consumption amount over 50 hours

incubation. (D) Dynamics of $\mathrm{CR}_{\mathrm{CO}_2}$ calculated from cumulative $Q_m$ and $CO_2$ evolution amount over 50 hours incubation.

# 4. Discussion

This study demonstrates the successful integration of a $CO_2$ sensor into IMC, exemplified by the SCD41 sensor and the TAM Air system. The integration of the SCD41 sensor into the IMC enables simultaneous quantification of heat and $CO_2$ flux from the same soil sample, even with minimum sample volume. This innovation addresses challenges associated with soil heterogeneity, enabling robust and continuous monitoring of heat and $CO_2$ dynamics. Such an approach supports the real-time calculation of key derived parameters, including CR, $\mathrm{CR}_{\mathrm{O}_2}$ and RQ, thereby providing a dynamic framework to interpret C and E fluxes over the incubation period.

Validation experiments demonstrated a neglectable influence of the sensor on the determination of $Q_m$ for both non- and glucose-amended soil treatment, affirming the reliability and non-invasive nature of this integrated system for monitoring $CO_2$ and $P_m$. Compared to methods using $CO_2$ trapping solution (Barros et al., 2011; Yang et al., 2024), the sensor-based integration avoids interference with microbial activities due to almost complete elimination of $CO_2$ from the gas phase. However, very high $CO_2$ partial pressures (>100 hPa, approx. 9.87%) in the headspace may also inhibit microbial growth (Onken and Liefke, 1989). The final percentage of $CO_2$ in our measurement was approximately 3% while the remaining $O_2$ in the air space was around 18%. However, this $CO_2$ level is below a concentration that is typically expected to have an influence on the metabolic activity of the soil microbial community. The relationship between $CO_2$ concentration and microbial growth rate, however, is highly dependent on soil properties, the chemical compositions of the substrate (relevant to energy content), and the degradability and availability of the substrates, which cannot be conclusively determined by this single study (Blagodatskaya et al., 2010). The system developed in this study allows investigations to elucidate this relationship for different soils and substrates.

Another important feature of our system is its capability for continuous and real-time measurements. This facilitates the analysis of dynamic and growth-phase specific metabolic CR parameters, offering significant advantages over end-point measurements (Herrmann and Bölscher, 2015) or discontinuous set-ups and discrete measurements which analyse heat and $CO_2$ in separate replicates (Endress et al., 2024; Wirsching et al., 2025; Yang et al., 2025). Compared to twin-flow systems for $CO_2$ and $O_2$ measurement (Griddle et al., 1990), the integrated $CO_2$-sensor in IMC offers a more streamlined and efficient design, requiring only a single measurement channel and eliminating the need for connecting the calorimeter vials to external sensors or tubing which bear the risk of thermal bridges introducing bias and increased variation in the measurements. By omitting the use of NaOH as $CO_2$ trap, the system avoids limitation associated with $NaHCO_3$ formation, as well as potential disturbance of $P_m$ measurements during NaOH replenishment, extended equilibrium settings and abrupt

reductions in $P_m$ due to the opening of the channels (Barros et al., 2017; Barros Pena, 2018; Griddle et al., 1991). Still, prolonged experiments at high aerobic microbial activities would require regular aeration, introducing disturbances by opening the vials (Yang et al., 2024).

However, the evaluation of $P_m$ with the presence of the SCD41 sensor was more complex than standard treatments, primarily due to the significant heat disturbance caused by the sensor' IR operation at a 15-minute interval. We selected a relatively long-time interval for $CO_2$ measurements compared to the $P_m$ measurements in order to minimise the thermal disturbance by the operation of the sensor and to have a characteristic frequency for signal filtering. The necessary signal processing to suppress these disturbances included FFT filtering.

As depicted in **Fig. 2**B, the error of $P_m$ for glucose-amended soil after 30 hours increased threefold compared to the treatment without sensor. This became particularly evident during the later stages of incubation when metabolic activity has diminished while the heat release by the sensor remains constant. The disturbance in the later phase can be attributed to two factors. Firstly, variability between replicates due to soil heterogeneity and uneven substrate distribution may increase measuring error as reported by Endress et al. (2024b), especially for glucose-amended soil. Second, the SCD41 sensor, as an IR-based sensor, generated a consistent intrinsic heat output of $1.6 \pm 0.3$ mW, which by far exceeded the maximum metabolic $P_m$ from the soil in this experimental setup (SM **Figure S1**B). This highlights the impact of the sensor's intrinsic heat generation on the calorimetric measurements and the necessity of careful signal processing. Further efforts will therefore be made in future to reduce the heat output of the $CO_2$ sensor. Another issue can arise in soils with high $CO_2$ production or with large sample quantities. The upper sensor detection value is 5% by volume. To address these challenges in future developments, an improved flow-through system incorporating an air-pump and placing sensor-integrated ampoules externally of TAM Air is proposed. This design would enlarge the soil sample capacity while minimizing the influence of the sensor's heat output on calorimetric accuracy.

RQ has been commonly used to evaluate microbial activities in soil and to study soil metabolism processes (Dilly, 2001). However, in practice, RQ varies depending on the metabolized substrate compositions (sugars ~1, proteins ~0.67-1.01, lipids ~0.68-0.80 organic acids ~0.97-4.2, Hicks Pries et al., 2020), environmental conditions, and nutrient levels. In our study, the RQ significantly exceeded 1 throughout the entire incubation period. Under aerobic degradation of carbohydrates such as glucose, the RQ is theoretically equal to 1. In our experiments, a slightly higher $CO_2$ production relative to $O_2$ consumption potentially indicates extra C mobilisation from SOM was observed, resulting in RQ of approximately 1.3–1.5. These findings align with values reported in previous studies for arable soil amended with glucose, where RQ ranged from 1.25 (Theenhaus et al., 1997) to as high as 1.6 or even greater (Dilly, 2001; Dilly and Zyakun, 2008), depending on different soil types. Several factors may explain the elevated RQ observed in this study. RQ greater than 1 can result from the use of alternative electron acceptors such as $NO_3^-$, the conversion of carbonates or organic acids,

379 which actively participate in the degradation of glucose input (Dilly, 2001, 2003; Endress et al.,
380 2024).

381 As predicted by the equation proposed by Hansen et al. (2004), $CR_{CO_2}$ should fall within the
382 range of 0-600 kJ mol$^{-1}$ $CO_2$. In our study, $CR_{CO_2}$ ranged from 247$\pm$133 kJ mol $CO_2$ $^{-1}$ to
383 358$\pm$249 kJ mol $CO_2$ $^{-1}$, aligning with the theoretical range mentioned and closely matching
384 experimental observations of 200 – 600 kJ mol $CO_2$ $^{-1}$ reported in previous studies (Wadsö et
385 al., 2004; Harris et al., 2012; Barros et al., 2016). Similarly, Endress et al (2024b) reported
386 $CR_{CO_2}$ equal to 344 kJ mol $CO_2$ $^{-1}$ at 50 hours for glucose-amended soil incubation. However,
387 in their study for $CR_{CO_2}$ dynamic, using the standard model, $CR_{CO_2}$ was predicted to firstly
388 stabilize from on 4 hours and then decline sharply at around 25 hours to approximately 250
389 kJ mol $CO_2$ $^{-1}$. When accounting for the delay caused by $CO_2$ diffusion and sorption into KOH
390 solution, the $CR_{CO_2}$ values matched more closely to experimental observations and also
391 previous studies (Yang et al., 2024). This finding confirms the potential impact of a 1.2 to 1.8
392 hours delay of $CO_2$ measurement, emphasizing the importance of correcting for the diffusion
393 effect, which can be addressed by our setup without the need for $CO_2$ absorption by alkaline
394 solutions and eliminate the reduction of $CO_2$ partial pressure. Therefore, the devices proposed
395 in this study could potentially eliminate the issue of $CO_2$ diffusion, providing $CR_{CO_2}$ dynamics
396 closely aligned to the standard model prediction.

397 Hansen et al. (2004) predicted $CR_{O_2}$ should always be equal to 455 kJ mol$^{-1}$ $O_2$ in aqueous
398 environment. Our observations of $CR_{O_2}$ (419$\pm$119 kJ mol $O_2$ $^{-1}$) aligned with the values (439
399 kJ mol$^{-1}$ $O_2$) found by Endress et al (2024b). Hansen et al. (2004) claimed that deviation of
400 $CR_{O_2}$ from 455 kJ mol$^{-1}$ $O_2$ can only occur under anaerobic conditions in aqueous solutions
401 with nonzero reaction enthalpy existing in the systems. However, continuous $O_2$ monitoring
402 in this study showed no strong indication of $O_2$ limitation or depletion, suggesting that the
403 experimental setup was largely aerobic and free from significant anaerobic interference.

## 404 5. Conclusion

405 This study demonstrates the successful integration of the SCD41 sensor into IMC, allowing
406 non-invasive, simultaneous measurement of heat and $CO_2$ flux from small arable soil samples.
407 By addressing challenges associated with soil heterogeneity and delayed detection due to $CO_2$
408 diffusion and supporting dynamic calculation of metabolic parameters alongside parallel $O_2$
409 measurement, the presented approach outperforms previous methods through minimizing
410 interference with microbial activities from reduced $CO_2$ partial pressure. In addition, the
411 suggested methodology is well-suited for high-throughput applications in soil analyses, as it is
412 compatible with multi-channel calorimeters such as the TAM IV-48 (TA Instruments, New
413 Castle, USA) or Symcel's 48-well calScreener (Symcel, Stockholm, Sweden), which are already
414 optimized for parallel sample analysis. The study validates the integrated setup as a reliable
415 and innovative tool for studying microbial activity and soil metabolism under aerobic
416 conditions while offering scalability and adaptability for broader experimental applications in
417 soil systems.

## CRediT authorship contribution statement

Shiyue Yang: Conceptualization, Methodology, Formal analysis, Investigation, Data curation, Visualization, Writing – original draft, Writing – Reviewing & Editing. Sven Paufler: Conceptualization, Methodology, Formal analysis, Investigation, Data curation, Writing – original draft, Writing – Reviewing & Editing. Hauke Harms: Supervision, Writing – review & editing. Anja Miltner: Supervision, Conceptualization, Methodology, Funding acquisition, Project administration, Writing – review & editing. Thomas Maskow: Supervision, Conceptualization, Methodology, Funding acquisition, Project administration, Writing – review & editing. Matthias Kästner: Supervision, Conceptualization, Methodology, Funding acquisition, Project administration, Writing – review & editing

## Declaration of competing interest

The authors declare that the research was conducted in the absence of any commercial or financial relationships that could be construed as a potential conflict of interest.

## Data availability

All raw and analysed data are available from authors upon reasonable request.

## Acknowledgements

The author(s) thanks for the funding by the Helmholtz-Centre for Environmental Research UFZ and the German Research Foundation (SPP2322: System ecology of soils – Energy Discharge Modulated by Microbiome and Boundary Conditions (SoilSystems)) with the projects TherMic (MI 598/9-1; MA 3746/8-1; MA 3746/8-2), DriverPool (MA 3746/9-1) and EnergyStructures (MA 3746/9-2). Schematics were created with BioRender. Soils were provided by S. J. Seidel and H. Hüging (University of Bonn, Germany). We wish to thank Hannah Riede (UFZ, Department of Microbial Biotechnology) for preliminary testing and all $CO_2$ sensor preparative work.

## References

Barros, N., Feijóo, S., 2003. A combined mass and energy balance to provide bioindicators of soil microbiological quality. Biophysical Chemistry 104, 561–572.

Barros, N., Feijóo, S., Hansen, L.D., 2011. Calorimetric determination of metabolic heat, CO2 rates and the calorespirometric ratio of soil basal metabolism. Geoderma 160, 542–547. doi:10.1016/j.geoderma.2010.11.002

Barros, N., Feijoo, S., Pérez-Cruzado, C., Hansen, L.D., Barros, N., Feijoo, S., Pérez-Cruzado, C., Hansen, L.D., 2017. Effect of soil storage at 4 °C on the calorespirometric measurements of soil microbial metabolism. AIMS Microbiology 3, 762–773. doi:10.3934/microbiol.2017.4.762

Barros, N., Feijóo, S., Simoni, J.A., Airoldi, C., Ramajo, B., Espina, A., García, J.R., 2008. A mass and energy balance to provide microbial growth yield efficiency in soil: Sensitivity to

metal layering phosphates. Journal of Thermal Analysis and Calorimetry 93, 657–665. doi:10.1007/s10973-007-8871-4

Barros, N., Hansen, L.D., Piñeiro, V., Pérez-Cruzado, C., Villanueva, M., Proupín, J., Rodríguez-Añón, J.A., 2016. Factors influencing the calorespirometric ratios of soil microbial metabolism. Soil Biology and Biochemistry 92, 221–229. doi:10.1016/j.soilbio.2015.10.007

Barros Pena, N., 2018. Calorimetry and soil biodegradation: Experimental procedures and thermodynamic models, in: Toxicity and Biodegradation Testing. Springer, pp. 123–145.

Blagodatskaya, E., Blagodatsky, S., Dorodnikov, M., Kuzyakov, Y., 2010. Elevated atmospheric CO2 increases microbial growth rates in soil: Results of three CO2 enrichment experiments. Global Change Biology 16, 836–848. doi:10.1111/j.1365-2486.2009.02006.x

Chakrawal, A., Herrmann, A.M., Manzoni, S., 2021. Leveraging energy flows to quantify microbial traits in soils. Soil Biology and Biochemistry 155, 108169. doi:10.1016/j.soilbio.2021.108169

Cooley, J.W., Tukey, J.W., 1965. An algorithm for the machine calculation of complex fourier series. Mathematics of Computation 19, 297–301. doi:10.1090/S0025-5718-1965-0178586-1

Criddle, R.S., Breidenbach, R.W., Rank, D.R., Hopkin, M.S., Hansen, L.D., 1990. Simultaneous calorimetric and respirometric measurements on plant tissues. Thermochimica Acta 172, 213–221. doi:10.1016/0040-6031(90)80576-K

Dilly, O., 2003. Regulation of the respiratory quotient of soil microbiota by availability of nutrients. FEMS Microbiology Ecology 43, 375–381. doi:10.1111/j.1574-6941.2003.tb01078.x

Dilly, O., 2001. Microbial respiratory quotient during basal metabolism and after glucose amendment in soils and litter. Soil Biology and Biochemistry 33, 117–127. doi:10.1016/S0038-0717(00)00123-1

Dilly, O., Zyakun, A., 2008. Priming Effect and Respiratory Quotient in a Forest Soil Amended with Glucose. Geomicrobiology Journal 25, 425–431. doi:10.1080/01490450802403099

Endress, M.-G., Dehghani, F., Blagodatsky, S., Reitz, T., Schlüter, S., Blagodatskaya, E., 2024. Spatial substrate heterogeneity limits microbial growth as revealed by the joint experimental quantification and modeling of carbon and heat fluxes. Soil Biology and Biochemistry 197, 109509. doi:10.1016/j.soilbio.2024.109509

Fricke, C., Lodovico, E.D., Meyer, M., Maskow, T., Schaumann, G.E., 2024. Design, calibration and testing of a novel isothermal calorespirometer prototype. Thermochimica Acta 738, 179785. doi:10.1016/j.tca.2024.179785

Gnaiger, E., n.d. Chapter 11.3 The Twin-Flow Microrespirometer and Simultaneous Calorimetry.

Griddle, R.S., Fontana, A.J., Rank, D.R., Paige, D., Hansen, L.D., Breidenbacht, R.W., n.d. Simultaneous measurement of metabolic heat rate, CO, production, and 0, consumption by microcalorimetry.

Hansen, L.D., Macfarlane, C., McKinnon, N., Smith, B.N., Criddle, R.S., 2004. Use of calorespirometric ratios, heat per CO2 and heat per O2, to quantify metabolic paths and energetics of growing cells. Thermochimica Acta, Energetics of Adaptation and Development: from molecular mechanisms to clinical practice 422, 55–61. doi:10.1016/j.tca.2004.05.033

Harris, J.A., Ritz, K., Coucheney, E., Grice, S.M., Lerch, T.Z., Pawlett, M., Herrmann, A.M., 2012. The thermodynamic efficiency of soil microbial communities subject to long-term stress is lower than those under conventional input regimes. Soil Biology and Biochemistry 47, 149–157. doi:10.1016/j.soilbio.2011.12.017

Herrmann, A.M., Bölscher, T., 2015. Simultaneous screening of microbial energetics and CO2 respiration in soil samples from different ecosystems. Soil Biology and Biochemistry 83, 88–92. doi:10.1016/j.soilbio.2015.01.020

Herrmann, A.M., Coucheney, E., Nunan, N., 2014. Isothermal Microcalorimetry Provides New Insight into Terrestrial Carbon Cycling. Environmental Science & Technology 48, 4344–4352. doi:10.1021/es403941h

Hicks Pries, C., Angert, A., Castanha, C., Hilman, B., Torn, M.S., 2020. Using respiration quotients to track changing sources of soil respiration seasonally and with experimental warming. Biogeosciences 17, 3045–3055. doi:10.5194/bg-17-3045-2020

Hirsch, R., 2024. Introduction to R, in: Hirsch, R. (Ed.), Analysis of Epidemiologic Data Using R. Springer Nature Switzerland, Cham, pp. 1–12. doi:10.1007/978-3-031-41914-0_1

Jing, Y., Miltner, A., Eggen, T., Kästner, M., Nowak, K.M., 2022. Microcosm test for pesticide fate assessment in planted water filters: 13C,15N-labeled glyphosate as an example. Water Research 226, 119211. doi:10.1016/j.watres.2022.119211

Kabwe, L.K., Hendry, M.J., Wilson, G.W., Lawrence, J.R., n.d. Quantifying CO2 ¯uxes from soil surfaces to the atmosphere.

Kästner, M., Maskow, T., Miltner, A., Lorenz, M., Thiele-Bruhn, S., 2024. Assessing energy fluxes and carbon use in soil as controlled by microbial activity - A thermodynamic perspective A perspective paper. Soil Biology and Biochemistry 193, 109403. doi:10.1016/j.soilbio.2024.109403

Lorenz, M., Blagodatskaya, E., Finn, D., Fricke, C., Hüging, H., Kandeler, E., Kaiser, K., Kästner, M., Lechtenfeld, O., Marhan, S., Maskow, T., Mayer, J., Miltner, A., Normant-Saremba, M., Poll, C., Resseguier, C., Rupp, A., Schrumpf, M., Schweitzer, K., Simon, C., Tebbe, C., Yang, S., Yousaf, U., Thiele-Bruhn, S., 2024. Database for the Priority Program 2322 SoilSystems – Soils and substrates used in the first phase (2021-2024). doi:10.5281/zenodo.11207502

Manzoni, S., Taylor, P., Richter, A., Porporato, A., Ågren, G.I., 2012. Environmental and stoichiometric controls on microbial carbon-use efficiency in soils. New Phytologist 196, 79–91. doi:10.1111/j.1469-8137.2012.04225.x

Maskow, T., Paufler, S., 2015. What does calorimetry and thermodynamics of living cells tell us? Methods 76, 3–10. doi:10.1016/j.ymeth.2014.10.035

Nordgren, A., 1988. Apparatus for the continuous, long-term monitoring of soil respiration rate in large numbers of samples. Soil Biology and Biochemistry 20, 955–957. doi:10.1016/0038-0717(88)90110-1

Onken, U., Liefke, E., 1989. Effect of total and partial pressure (oxygen and carbon dioxide) on aerobic microbial processes, in: Bioprocesses and Engineering. Springer, Berlin, Heidelberg, pp. 137–169. doi:10.1007/BFb0009830

Rowell, M.J., 1995. Colorimetric method for CO2 measurement in soils. Soil Biology and Biochemistry 27, 373–375. doi:10.1016/0038-0717(94)00218-P

Satienperakul, S., Cardwell, T.J., Cattrall, R.W., McKelvie, I.D., Taylor, D.M., Kolev, S.D., 2004. Determination of carbon dioxide in gaseous samples by gas diffusion-flow injection. Talanta 62, 631–636. doi:10.1016/j.talanta.2003.09.008

Sinsabaugh, R.L., Manzoni, S., Moorhead, D.L., Richter, A., 2013. Carbon use efficiency of microbial communities: stoichiometry, methodology and modelling. Ecology Letters 16, 930–939. doi:10.1111/ele.12113

Theenhaus, A., Maraun, M., Scheu, S., 1997. Substrate-induced respiration in forest and arable soils measured by O2-microcompensation: moisture conditions and respiratory quotient. Pedobiologia 41, 449–455. doi:10.1016/S0031-4056(24)00315-9

Tiemann, L.K., Billings, S.A., 2011. Changes in variability of soil moisture alter microbial community C and N resource use. Soil Biology and Biochemistry, 19th International Symposium on Environmental Biogeochemistry 43, 1837–1847. doi:10.1016/j.soilbio.2011.04.020

Wadsö, L., 2015. A method for time-resolved calorespirometry of terrestrial samples. Methods 76, 20–26. doi:10.1016/j.ymeth.2014.10.001

Wadsö, L., Hansen, L.D., 2015. Calorespirometry of terrestrial organisms and ecosystems. Methods 76, 11–19. doi:10.1016/j.ymeth.2014.10.024

Wadsö, L., Li, Y., Bjurman, J., 2004. Measurements on two mould fungi with a calorespirometric method. Thermochimica Acta 422, 63–68. doi:10.1016/j.tca.2004.05.034

Wirsching, J., Endress, M.-G., Di Lodovico, E., Blagodatsky, S., Fricke, C., Lorenz, M., Marhan, S., Kandeler, E., Poll, C., 2025. Coupling energy balance and carbon flux during cellulose degradation in arable soils. Soil Biology and Biochemistry 202, 109691. doi:10.1016/j.soilbio.2024.109691

Wolcott, C.A., Campbell, C.T., 2015. Method for direct deconvolution of heat signals in transient adsorption calorimetry. Surface Science 633, 17–23. doi:10.1016/j.susc.2014.11.005

Yang, S., Di Lodovico, E., Rupp, A., Harms, H., Fricke, C., Miltner, A., Kästner, M., Maskow, T., 2024. Enhancing insights: exploring the information content of calorespirometric ratio in dynamic soil microbial growth processes through calorimetry. Frontiers in Microbiology 15, 1321059. doi:10.3389/fmicb.2024.1321059

Yang, S., Rupp, A., Kästner, M., Harms, H., Miltner, A., Maskow, T., 2025. Experimental access to cellulose oxidation and the dynamics of microbial carbon and energy use in artificial soil under varying temperature, water content, and C/N ratio. Soil Biology and Biochemistry 203, 109717. doi:10.1016/j.soilbio.2025.109717

Yoshizawa, T., Hirobayashi, S., Misawa, T., 2011. Noise reduction for periodic signals using high-resolution frequency analysis. EURASIP Journal on Audio, Speech, and Music Processing 2011, 5. doi:10.1186/1687-4722-2011-426794

# Supplementary Materials

# An Integrated Measurement of Microbial Heat and CO2 Evolution (Calorespirometric Ratio) in Soil Using an Established Isothermal Microcalorimeter Coupled with a $CO_2$ Sensor

Shiyue Yang[1], Sven Paufler[1], Hauke Harms[2], Matthias Kastner[3], Anja Miltner[3], Thomas Maskow[1*]

[1]Department of Microbial Biotechnology, Helmholtz-Centre for Environmental Research – UFZ, Permoserstraße 15, 04318 Leipzig, Germany

[2]Department of Applied Microbial Ecology, Helmholtz-Centre for Environmental Research – UFZ, Permoserstraße 15, 04318 Leipzig, Germany

[3]Department of Molecular Environmental Biotechnology, Helmholtz-Centre for Environmental Research – UFZ, Permoserstraße 15, 04318 Leipzig, Germany

## S1 detailed information about SCD41 – infrared $CO_2$ sensor

Sensirion SCD41 sensor (SCD41-D-R2) is an emerging IR sensor in the field of $CO_2$. The small size ($10.1 \times 10.1 \times 6.5$ mm$^3$) and large output range (0 ppm – 40000 ppm with accuracy of $\pm$ (40 ppm + 5%)) of the sensor enables the integration into other measuring techniques such as calorimeter. The accuracy and linearity of SCD41 is shown in **Figure S1**(C). Detailed information can be found on https://sensirion.com/products/catalog/SCD41. The SCD41 was used with the SCD-41 breakout board from Adafruit, providing I2C pull resistors and a linear voltage converter. To implement the communication protocol of the sensor on the microcontroller, the respective Sensirion libraries for the Arduino platform were employed.

## S2 Gas leaking rate in stainless-steel ampoule and disturbance from SCD41 sensor

To ensure the gas tightness of stainless-steel ampoules. One proving experiment was conducted by injecting mixed air with around 2% $CO_2$ into the ampoule and ran over 200 hours. The gas leaking rate was calculated by linear regression of remaining $CO_2$ concentration versus time. Meanwhile, the same ampoule was inserted into the TAM Air for heat production rate monitoring for sensor noise baseline determination. As shown in **Figure S1**(A), after injection, $CO_2$ dropped from approx. 2.2% to approx. 2.1% after 200 hours and thus the leaking rate is approximately 0.00045% h$^{-1}$ which is considered as negligible in our data analysis. Continuously monitored $P_m$ remained mostly constant during the entire time period and demonstrated the mean value of 1.6 $\pm$ 0.3 mW which is used for baseline correction for data analysis of soil incubations.

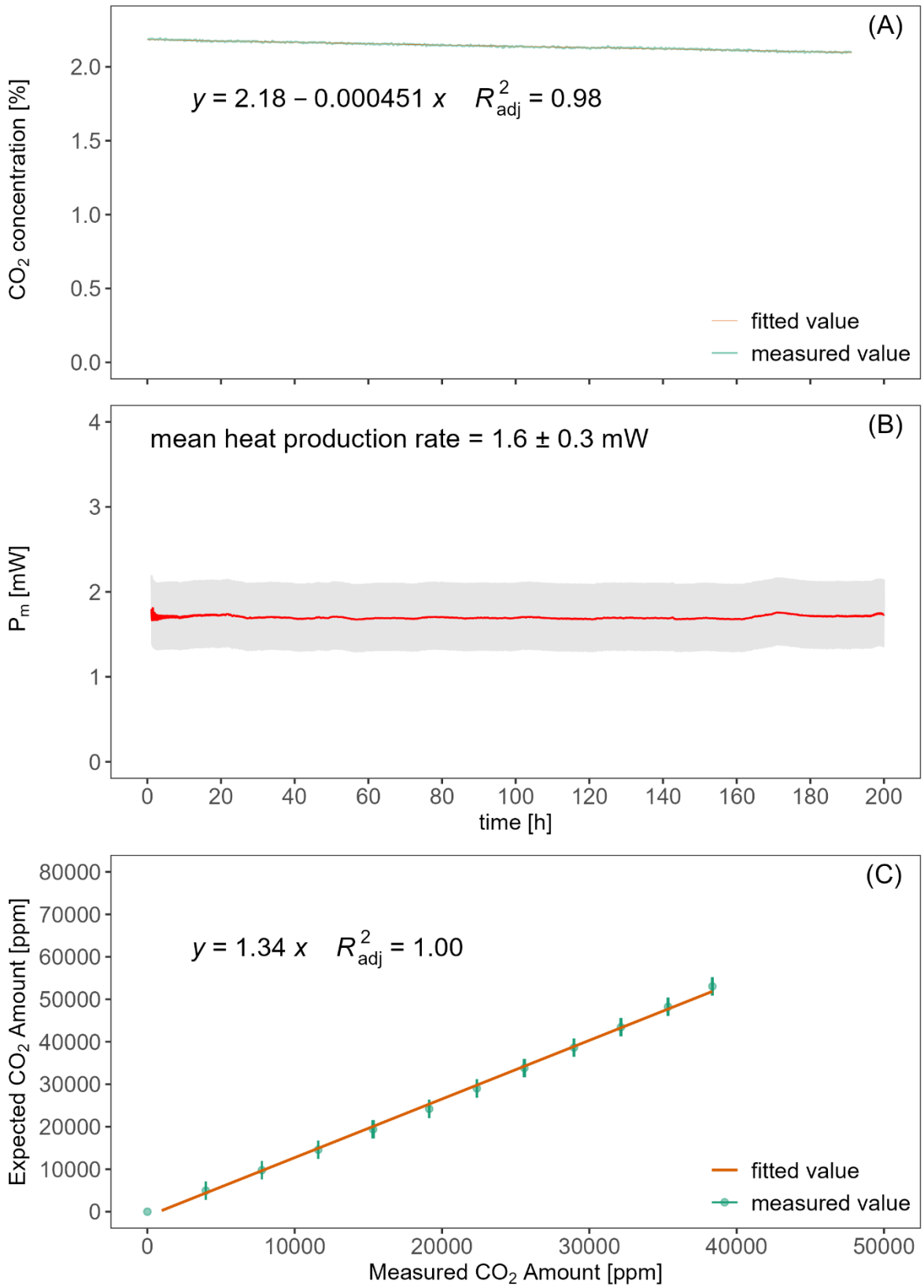


626

627 **Figure S1** $CO_2$ concentration over 200 hours' measurement with fixed amount of $CO_2$ injection
628 inside sealed stainless-steel ampoule (A), the corresponding $P_m$ under 20 °C (B) and linearity
629 of SCD41 measurement results when compared to real $CO_2$ amount. A linear regression was
630 used in (A) to determine the average leaking rate of $CO_2$. Grey points are direct measured

values of $P_m$ with sensor mounted on top of the stainless-steel lid while red lines are values smoothed and converted with FFT and IFFT smoothing method. The mean $P_m$ is approximately 1.6±0.3 mW. (C)

## S3 Theoretical framework

The metabolic $P_m(t)$ is the difference between $P_{SG}(t)$ and $P_S(t)$ (**Eq.** (S1)). $P_{SG}(t)$ is the heat production rate of glucose-amended soil and $P_s(t)$ is the heat production rate of non-amended soil.

$$P_m(t) = P_{SG}(t) - P_s(t) \qquad \textbf{Eq.}\ (S1)$$

The metabolic $Q_m(t)$ is the difference between $Q_{SG}(t)$ and $Q(t)$ (**Eq.** (S2)). $Q_{SG}(t)$ is the total heat production of glucose-amended soil and $Q_s(t)$ is the total heat production non-amended soil.

$$Q_m(t) = Q_{SG}(t) - Q_s(t) \qquad \textbf{Eq.}\ (S2)$$

The volume of air space was calculated as the difference between the ampoule volume and the volume of water and dry soil particles. $V_{CO_2}$ is calculated as show in **Eq.** (S3):

$$V_{CO_2} = \frac{CO_2[ppm]}{10^6} \cdot \left(V_{ampoule} - V_{water} - V_{soil\ particle}\right) \qquad \textbf{Eq.}\ (S3)$$

In **Eq.** (S3), $V_{ampoule}$, $V_{water}$ and $V_{soil\ particle}$ stands for the volume of stainless-steel ampoule (20mL as nominal volume and 25 mL as the real volume), water contained in the soil and dry soil particle, respectively.

$V_{O_2}$ is calculated as show in **Eq.** (S4):

$$V_{O_2} = (O_2(t_0) - O_2(t)) \cdot \left(V_{vessel} - V_{water} - V_{soil\ particle}\right) \qquad \textbf{Eq.}\ (S4)$$

In **Eq.** (S4), $O_2(t_0) - O_2(t)$ is the difference in $O_2$ saturation between beginning point ($t_0$) and time = t in the unit of %. $V_{vessel}$ is the volume of $O_2$ measuring vessel which equals to 60 mL (real volume and nominal volume as 50 mL).

## S4 FFT filter method for denoising

The FFT filtering method is proven to be an effective tool for denoising periodic disturbances (Yoshizawa et al., 2011; Wolcott and Campbell, 2015). In our experiments, the SCD41 sensor measured $CO_2$ saturation [ppm] at 15-minute intervals. Every 15 minutes the sensor was switched into "singal-shot" measuring mode for three consecutive measurements within about 30 seconds for averaging then going idle for the remaining time in the 15 minutes cycle. The increased sensors' power consumption during the 30 seconds active measurement resulted in a very regular calorimetric noise pattern. The $P_m$ was exported with a 5 second interval. Thus, the FFT method was applied to each $P_m(t)$ data set to obtain the frequency domain representation ($P_{FFT}(t)$ using **Eq.** (S5)). The power spectrum ($I$) of the corresponding dataset was calculated by squaring the magnitude of the FFT and normalized by the total length of the measuring time ($\Delta t$). A frequency factor ($f$) was generated manually (**Eq.** (S7)), representing the frequency axis corresponding to the FFT results. The cutoff frequency was

chosen based on the desired filtering characteristics. The index corresponding to this cutoff frequency was identified by finding the minimum absolute difference between the frequency vector and the cutoff value. To perform denoising, a zero operation was applied to the FFT coefficients corresponding to frequencies higher than the cutoff. The inverse FFT (**Eq.** (S8)) was then computed on the modified FFT coefficients to reconstruct the denoised signal in the time domain and the denoised signal was normalized by dividing the total number of samples ($n$).

$$P_{FFT}(t) = FFT(P_m(t)) \quad \textbf{Eq.} \text{ (S5)}$$

$$I = \frac{abs(P_{FFT}(t))^2}{\Delta t} \quad \textbf{Eq.} \text{ (S6)}$$

$$f = 0{:}\frac{\Delta t - 1}{\Delta t} \quad \textbf{Eq.} \text{ (S7)}$$

$$P_{IFFT}(t) = \frac{IFFT\left(P_{FFT}(t)\right)}{n} \quad \textbf{Eq.} \text{ (S8)}$$

## S5 Statistical results

The one-way Anova method was used to check the influence of sensor disturbance on heat production rate measurement for both blank and glucose-amended soil.

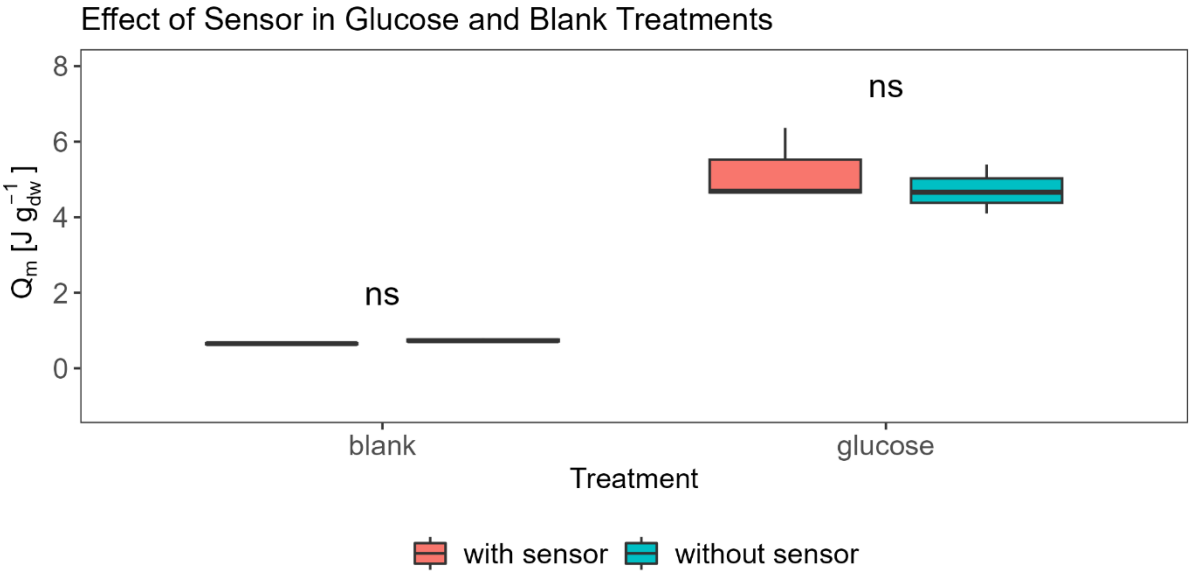


**Figure S2** Effect of sensor disturbance on glucose-amended and non-amended soil. No significant difference was observed between systems with and without sensor, neither for glucose-amended nor for non-amended soil. The average of $Q_m$ for non-amended soil is around 1 J $g_{dw}^{-1}$ (left) and 5 J $g_{dw}^{-1}$ for glucose-amended soil (right) at 50 hours.

678 **S6 Ambient temperature and bath temperature in TAM Air**

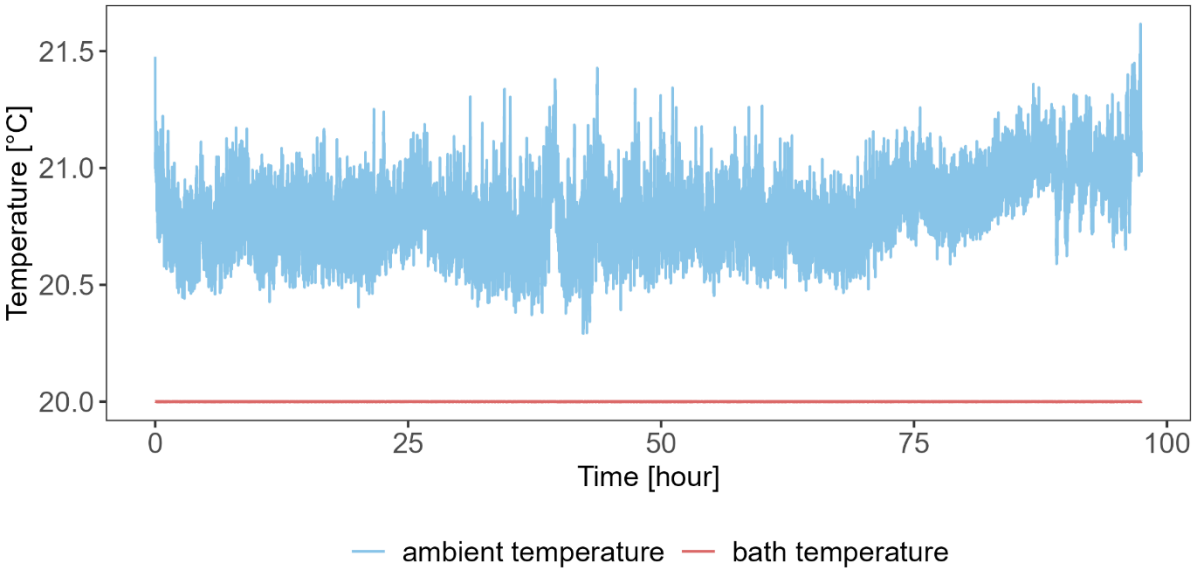


679

680 **Figure S3** Comparison of ambient temperature (light blue curve, 20.8±0.2 °C) and bath
681 temperature inside of TAM Air (20.0±0.0003 °C)